Preparation, characterization and dyeing wastewater treatment of a new PVDF/PMMA five-bore UF membrane with β-cyclodextrin and additive combinations

Xiaozheng Bian, Jianping Huang, Lin Qiu, Chunyan Ma and Danli Xi

ABSTRACT

A new type of polyvinylidene fluoride (PVDF)/polymethyl methacrylate (PMMA) hollow fiber membrane (HFM) with five bores was prepared. The effects of polyvinylpyrrolidone (PVP), β-cyclodextrine (β-CD), polyethylene glycol (PEG) and polysorbate 80 (Tween 80) and their combinations on the PVDF/PMMA five-bore HFMs were investigated. The performance and fouling characteristics of five-bore HFMs for dyeing wastewater treatment were evaluated. Results indicated that adding 5 wt.% PVP increased the porosity and water flux of the membrane but decreased the bovine serum albumin (BSA) rejection rate. Adding 5 wt.% β-CD significantly improved the tensile strength and rejection of the HFMs with no effect on the increase of water flux. The characteristic of the HFMs with different additive combinations proved that the mixture of 5 wt.% PVP and 1 wt.% β-CD gave the best membrane performance, with a pure water flux of 427.9 L/ m^2·h, a contact angle of 25°, and a rejection of BSA of 89.7%. The COD_{cr} and UV_{254} removal rates of dyeing wastewater treatment were 61.10% and 50.41%, respectively. No breakage or leakage points were found after 120 days of operation, showing their reliable mechanical properties. We set the operating flux to 55 L/m^2·h and cross-flow rate to 10%, which can effectively control membrane fouling.

Key words | additive, β-cyclodextrine (β-CD), dyeing wastewater, five-bore, hollow fiber membrane, polyvinylpyrrolidone (PVP)

HIGHLIGHTS

- PVDF/PMMA five-bore HFMs were prepared by dry-wet spinning.
- The addition of PVP and β-CD had significant effects on HFM hydrophilicity and rejection respectively.
- The best film properties were obtained by mixing 5 wt% PVP and 1 wt% β-CD.
- The laboratory-made membrane module could effectively remove chemical oxygen demand and the turbidity of the dyeing wastewater.
- No breakage or leakage points were found after 120 days of operation, showing their reliable mechanical properties.

Xiaozheng Bian
Lin Qiu
School of Water Conservancy,
North China University of Water Resources and Electric Power,
Zhengzhou 450046,
China

Jianping Huang (corresponding author)
Ural Institution,
North China University of Water Resources and Electric Power,
Zhengzhou 450045,
China
E-mail: *huangjianpingh@163.com*

Chunyan Ma
Danli Xi
Donghua University,
Shanghai 200051,
China

doi: 10.2166/wst.2021.104

GRAPHICAL ABSTRACT

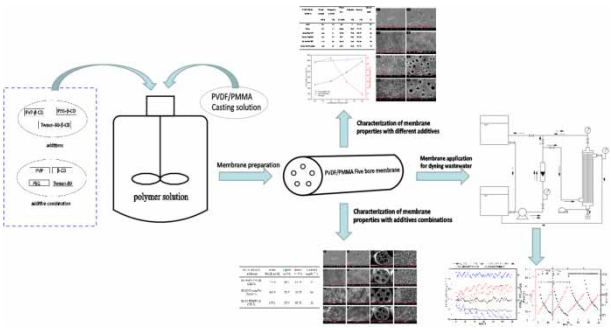

INTRODUCTION

Polyvinylidene fluoride (PVDF) is widely used in wastewater treatment due to its outstanding mechanical and chemical properties (Khayet *et al.* 2002; Liu *et al.* 2011; Kang & Cao 2014). However, its hydrophobicity usually causes membrane fouling in water and wastewater treatment, thereby increasing its application cost (Loukidou & Zouboulis 2001; Bagheri & Mirbagheri 2018). Many studies have focused on the hydrophobic modification of PVDF, among which blending is a simple and practical method in large-scale membrane preparation (Liu *et al.* 2009; Aid *et al.* 2019).

Polymethyl methacrylate (PMMA) is most commonly used for PVDF modification due to the cost and performance advantages (Huang & Zhang 2004). Studies (Okabe *et al.* 2010; Ma *et al.* 2013) have demonstrated that mixing PMMA with PVDF can significantly improve the hydrophilicity of the membranes, but that the retention rate of bovine serum albumin (BSA) remains unchanged. The addition of PMMA changes the film-forming structure and increases the size of finger-like pore. Even so, the PVDF/PMMA blended membrane still exhibits a similar surface and cross-sectional structure to the PVDF membrane, and its performance improvement depends on the concentration of PMMA (Rajabzadeh *et al.* 2012; Aid *et al.* 2019).

Therefore, some hydrophilic additives are usually used to adjust the membrane structure to improve the final membrane performance during the phase inversion, such as polyvinylpyrrolidone (PVP) (Wu *et al.* 2006; Zhou & Xi 2008; Simone *et al.* 2010; Bi *et al.* 2012), polyethylene glycol (PEG) (Xu & Xu 2002; Chakrabarty *et al.* 2008; Wongchitphimon *et al.* 2011; Rajabzadeh *et al.* 2012), polysorbate 80 (Tween 80) (Amirilargani *et al.* 2009; Chang *et al.* 2014) and β-cyclodextrine (β-CD) (Huang *et al.* 2009; Wu *et al.* 2013; Yu *et al.* 2015; Wang *et al.* 2019). PVP is a good pore-forming agent, and can improve the hydrophilicity and enhance the toughness of membrane (Marchese *et al.* 2003; Zhou & Xi 2008). PVDF thermal phase separation membrane with PVP can significantly improve the maximum stress, elongation, and hydrophilicity of the membranes (Rajabzadeh *et al.* 2012). Wu *et al.* (2006) prepared a film with 5 wt.% PVP, which produced a thinner epidermis and inclined finger-like pores in the membrane. As for β-CD, it has a special structure of internal hydrophobicity and external hydrophilicity (Crini 2014; Liu *et al.* 2020; Zhao & Sillanpää 2020). β-CD has been extensively adopted as the adsorbent for organic compounds due to its low cost and moderate cavity size (Liu *et al.* 2020). It can easily aggregate polymers to form a macromolecular network, thereby improving membrane hydrophilicity, strength, and rejection (Gao *et al.* 2019; Rahimi *et al.* 2020). β-CD can also improve the water purification capacity of the membrane and has excellent potential for removing pollutants (Alsbaiee *et al.* 2016). In addition, PEG and Tween 80 are also used as pore-forming agents in polymeric membranes. With the increasing molecular weight of PEG, the membrane porosity and pure water flux increased, and the mechanical strength and retention rate decreased gradually (Xu & Xu 2002). When Tween 80 was used as a surfactant additive to prepare polyethersulfone (PES) flat membranes, adding a small amount (4 wt.%) of Tween 80 increased the water content, porosity, and water permeability of the membrane (Amirilargani *et al.* 2009).

Conventional single-hole hollow fibre membranes (HFMs) (Yin *et al.* 2013) may break and become entangled during water treatment (Pan *et al.* 2013; Zhang *et al.* 2015). To resolve the mechanical durability issue, some researchers have developed membranes with special structures and

shapes (Bu-Rashid & Czolkoss 2007; Peng *et al.* 2011) and proposed the idea of multi-channels (Zhang *et al.* 2006). At present, multi-channel polymer material membranes, such as PVDF, PES, and polyacrylonitrile (PAN), mainly include seven-bore, tri-bore, and five-bore membranes, which have been widely used in ultrafiltration (UF) (Peng *et al.* 2011; Wang *et al.* 2014; Wan *et al.* 2017; Back *et al.* 2019), forward osmosis (FO) (Luo *et al.* 2014; Li *et al.* 2015) and membrane distillation (MD) (Wang & Chung 2012; Lu *et al.* 2016).

The multi-bore HFM has a unique geometry with a high porosity and excellent mechanical strength (Wang & Chung 2012; Back *et al.* 2019). In the preparation process of the multi-channel PVDF UF HFM, the addition of hydrophilic materials or pore-forming agents can effectively improve the hydrophilicity and mechanical strength of the membrane, thereby improving its anti-pollution ability and durability for wastewater treatment. The PVDF/PEG seven-bore UF HFMs using PEG as a pore-forming agent increase the membrane hydrophilicity and water flux and improve the membrane durability and lifetime for wastewater treatment (Wan *et al.* 2017). Ma *et al.* (2012, 2016) prepared PVDF/PMMA/TPU five-bore HFMs. The addition of PMMA and TPU greatly increased the membrane pollutant removal performance and anti-pollution capability for dyeing wastewater treatment. In recent years, β-CD has received more and more attention as an adsorbent or additive in water treatment. A new adsorbent, nitrilotriacetic acid β-cyclodextrin-chitosan, was synthesized for the effective simultaneous removal of dyes and metals (Rahimi *et al.* 2020). A PVDF/PMMA five-bore HFM with β-CD can effectively remove polycyclic aromatic hydrocarbons (Huang *et al.* 2009). The β-CDP membranes have excellent adsorption performance and filtration advantages, and can remove organic micro-pollutants from water ultra-fast (Wang *et al.* 2019). However, it is rarely reported that β-CD was combined with other additives to prepared PVDF HFM for water treatment.

Previous work in our group has prepared a series of five-bore membranes, such as PVDF/PMMA/TUP, PVDF/PMMA/PVP, PVDF/PMMA/β-CD (Huang *et al.* 2009; Ma *et al.* 2012). Compared with single-bore HFMs, five-bore HFMs have better anti-pollution and pollutant removal characteristics when used in printing and dyeing wastewater treatment (Ma *et al.* 2016). Therefore, the objective of this study was to prepare five-hole PVDF/PMMA HFM by adding different additives and additive combinations. By measuring the morphological characteristics, mechanical properties, and physical properties of HFM, the influence of additives and their combinations on PVDF/PMMA five-bore HFM was explored. In addition, a membrane module was assembled for printing and dyeing wastewater treatment. The pollutant removal performance, anti-pollution and durability of the membrane were explored, and the operating conditions of the membrane process were determined.

MATERIALS AND METHODS

Chemicals and materials

PVDF was purchased from Shanghai 3F New Materials Co., LTD. PMMA explored was purchased from Heilongjiang Longxin Chemical Co., LTD. PVDF and PMMA are guaranteed reagent (GR). The solvent was *N*, *N*-dimethyl acetamide (DMAc) (AR) (Tianjin Ruijinte Chemical Co., LTD). The distilled water was non-solvent. BSA (MW67000, AR) was bought from Shanghai Boao Biotechnology Co., Ltd. PVP K30, β-CD, PEG1000, and Tween 80 were obtained from Sino-Pharm Chemical Reagent Co., Ltd (China). The additives were all analytical reagents.

Membrane preparation

Firstly, we dissolved a 17 wt.% polymer blend of PVDF/PMMA (80/20) in the solvent to prepare the casting solution. Then, we added a single additive to the casting solution: 5 wt.% PVP K30, 5 wt.% β-CD, 5 wt.% PEG1000 or 5 wt.% Tween 80 and combinations of additives: 5 wt.% PVP + 5 wt.% β-CD, 5 wt.% PEG + 5 wt.% β-CD and 5 wt.% Tween 80 + 5 wt.% β-CD. Each separate solution was stirred at 80 °C to form a homogeneous solution. The DMAc was used as the solvent. The casting solution was then kept in the dark for 24 hours and degassed before spinning. Finally, the modified hollow fiber UF membranes were prepared at room temperature by dry-wet spinning (Khayet *et al.* 2002).

The membranes prepared were of three types:

(1) PVDF/PMMA membranes without additive;
(2) PVDF/PMMA membranes with an additive (PVP, PEG1000, Tween 80, β-CD);
(3) PVDF/PMMA membranes with additive combinations (PVP-β-CD, PEG-β-CD, Tween 80-β-CD).

The spinning device is shown in Figure 1. The polymer solution reservoir was fitted with safety valve, heating device, nitrogen inlet and interface with vacuum pump. Part of the nitrogen in the reservoir could be manually adjusted to release, so the pressure in the tank could be

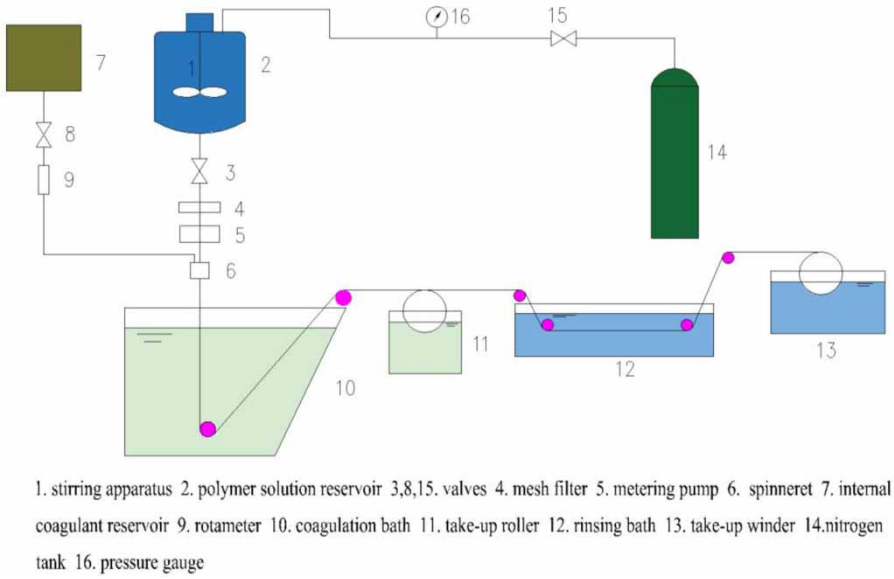

Figure 1 | Process flow chart of the hollow fiber membrane spinning system.

adjusted during spinning. The vacuum pump was used for vacuuming defoaming. In our experiment, the laboratory-made spinneret was five inner tubes, and the inner diameter of the spinneret orifice plate is shown in Figure 2. The diameter of the spinneret was 3.65 mm. The diameter of the five inner tubes on the spinneret was 0.42 mm, with a hole in the middle for the flow of the internal coagulation bath. The vertical distance between the center of the inner tube and the outer diameter of the spinneret was 0.76 mm. Driven by nitrogen pressure and a constant-flow pump, the casting solution passed through the orifice and inner fluid entered the inner tubes, respectively.

10% DMAc aqueous solution was used as the internal coagulation bath at 13 mL/min of flow, while water was used as the external coagulation bath, which flowed through the spinneret through the rotameter by gravity and was used to generate and control the porous structure of HFM. The air gap distance was 14 cm.

After spinning, the fiber was washed in distilled water for 48 hours to remove the residual DMAc solution. Then, to prevent the porous structure collapsing, we soaked it in 50% glycerin solution for 24 hours. Finally, we dried the membrane in ambient air.

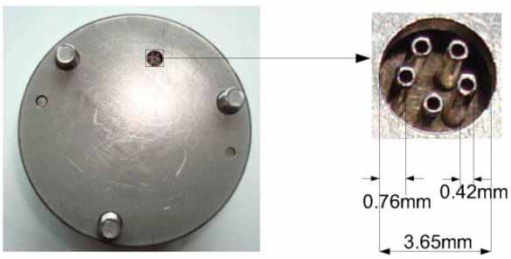

Figure 2 | The shape of spinneret.

Properties of membranes

Mechanical properties of membranes

The tensile strength and elongation of the membranes were measured using a tensile device (AG-1, Shimadzu, Japan). Tensile tests were carried out using a 100 mm gauge and 10 mm/min elongation speed.

Water flux (J_W) and retention rate (R) tests

Pure water was used to compress the membrane at 0.1 MPa for 30 min to drive out bubbles and obtain a steady state ultrafiltration membrane. At 0.1 MPa, water flux (J_W) was measured using a laboratory-made single filament membrane module. The test mode: three sections were randomly selected from the same batch of spinning membranes for the pure water flux test, and the average value was taken. For a certain type of membrane additive, three batches of water flux were measured, and finally the average value was calculated and recorded.

The retention rate of membranes was tested with 0.1 g/L BSA solution at 0.1 MPa. The feed and permeate concentration of BSA were detected by UV spectrophotometer (Shimadzu, Japan) at a wavelength of 280 nm. Equations (1) and (2) were used for calculating the water flux (J_W)

and retention (R) of the membranes, respectively (Chakrabarty *et al.* 2008; Bi *et al.* 2012). The test mode was the same as the water flux.

$$J_W = \frac{Q}{A} \tag{1}$$

$$R = \left(1 - \frac{C_P}{C_F}\right) \times 100\% \tag{2}$$

where J_W is the pure water flux of the membranes (L/m^2·h), Q is the volume of water passing through per unit time (L/h), A is the effective membrane area (m^2). R is the interception rate to the BSA solution (%), C_P and C_F are the feed of BSA concentration and permeate concentration, respectively (wt.%).

Membrane morphology

The cross-section morphology of the membrane was observed by scanning electron microscope (SEM) (JSM-5600LV, JEOL, Japan). First, the fibers were immersed in nitrogen for several minutes until the cross-section was exposed, then the membranes were sputtered with gold in a vacuum and tested under 10 kV at 20 °C.

Contact angle and porosity

The contact angle of the HFMs was determined by JY-82 automatic contact angle goniometer. We used double-sided tape to fix both sides of the membrane sample to ensure that the sample was flat. The porosity was determined by the dry-wet method and calculated using Equation (3).

$$\varepsilon = \frac{W_1 - W_2}{\left[\pi\left(\frac{D}{2}\right)^2 - 5.\left(\frac{d}{2}\right)^2\right] \cdot L \cdot \rho} \times 100\% \tag{3}$$

where, W_1 and W_2 are the wet weight and the dry weight of the membranes respectively, L is the length and D is the outer diameter of the membrane, d is the inner diameter of a single hole of the five holes, and ρ is the specific gravity of water.

Treatment of dyeing wastewater

Module production

The laboratory-made membrane module is shown in Figure 3. Four hundred hollow fibers with an effective length of 60 cm were installed in the module. The effective surface area of the membrane module was 1 m^2. The total diameter of the module was 15 cm. The sealant layer was potted with epoxy resin, and an aeration port was reserved at the bottom for aeration of the membrane module. The outlet end and dead end of the membrane module are also shown in the Figure 3. Sewage first entered the membrane module from the water inlet, then entered the internal water flow channel from the outside of the membrane to the inside, and finally flowed out of the water outlet. The concentrated water was discharged from the concentrated water outlet.

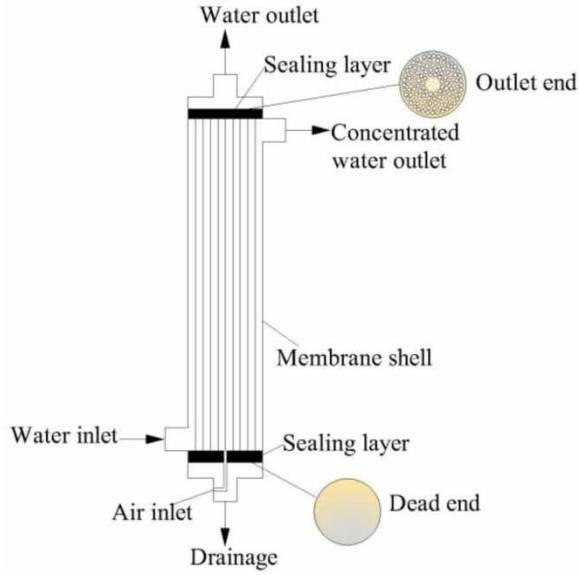

Figure 3 | The laboratory made membrane module.

Dyeing wastewater advanced treatment device and operation

The effluent from the secondary sedimentation tank of dyeing wastewater was further treated using the five-bore HFM module to evaluate the permeability and mechanical strength of the five-bore HFMs with additives. The influent of this device was from an improved AAO process system (Figure S1, Supplementary Information). The feed water of the AAO process system was synthetic wastewater. After treatment, the secondary effluent entered the advanced treatment device. The dyeing wastewater advanced treatment device is shown in Figure 4. ⑪ and ⑫ controlled the secondary outlet pump to ensure the liquid level of the ①. Then, sewage was transported to the inlet of the membrane module by ②. The influent was controlled by a

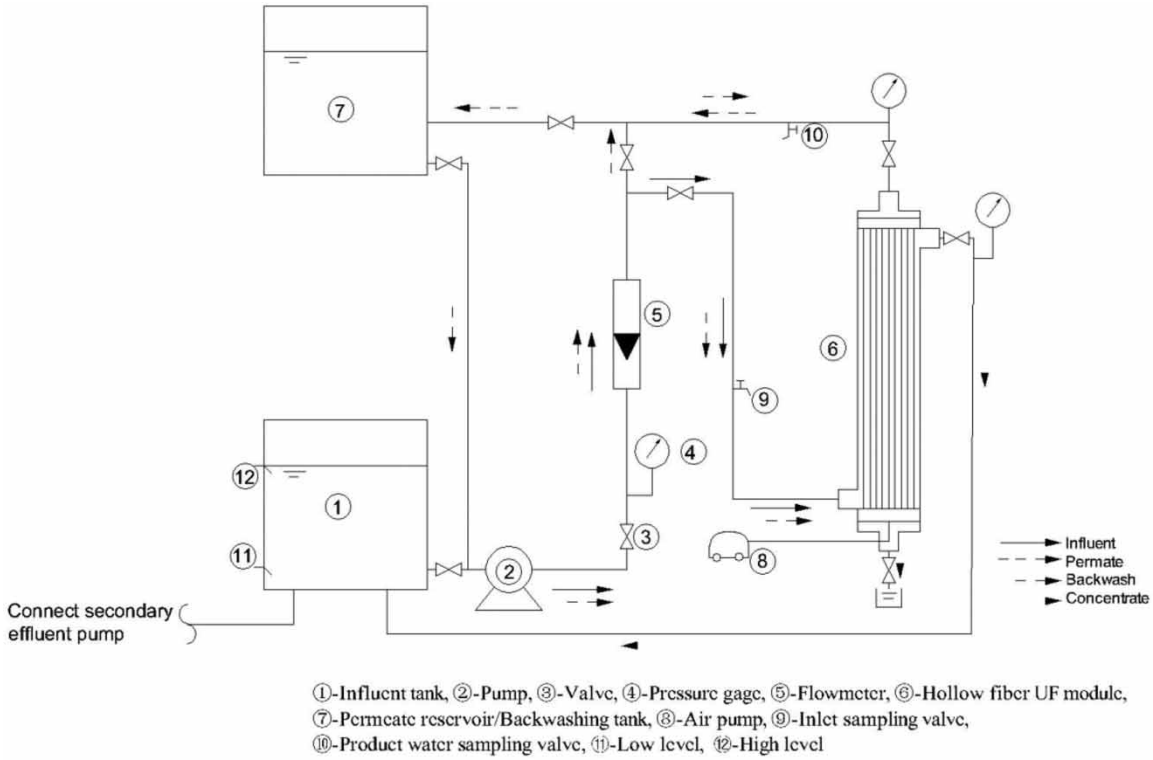

Figure 4 | Schematic of advanced treatment of dying wastewater.

programmable logic controller (PLC) system according to the process of operation. There were no large particles in the influent. The permeating liquid was produced at the water outlet of membrane and the concentrated water returned to ①. Water backwashing and aeration was carried out in each cycle. The operating procedure of the membrane was influent (effluent) for 50 min, aeration for 1 min, aeration and water backwashing for 1 min and draining for 30 seconds. The procedure was controlled by a PLC automatic control system and ran automatically in cycles. The effective area of the membrane module was 1 m^2. The average water yield was 42.85–52.4 L/h and the membrane flux was 45–55 litres/hour/m^2 (LMH). The transmembrane pressure (TMP) was calculated by measuring the pipeline using Equation (4).

$$TMP = \frac{(P_{\text{inf}} + P_{con})}{2} - P_{eff} \tag{4}$$

where P_{inf}, P_{con}, P_{eff} are the pressure of the water inlet, the concentrated water outlet, and the water outlet.

Parameter monitoring and water quality analysis

Samples were taken every 2 hours at the sampling valves ⑨ and ⑩. The sampling of the dye wastewater was 24 hour-mixed samples. The performance of pollutant removal was monitored each day by measuring chemical oxygen demand (COD), UV_{254} and dye concentration in the influent and effluent. COD was detected by quick-test method systems provided by Lianhua Co., Ltd. UV254 and dye concentration was measured via UV/VIS spectrophotometer under 254 and 598 nm. Pressure values were monitored and recorded via an online manometer on the pipeline. Turbidity and conductivity were measured by portable instruments HASH 2100Q and HASH, HQ14d respectively.

The membrane permeability test was the main method for chemical cleaning node judgment and long-term membrane service life analysis (Zhang *et al.* 2020). Membrane permeability was reflected by specific flux (SF), calculated as follows:

$$SF = \frac{J}{TMP} \tag{5}$$

where J represents membrane flux. In this test, the membrane flux J was maintained unchanged, and the TMP showed a trend of gradual increase with the continuous operation time of the membrane system. The test water temperature was relatively stable and maintained at 23–25 °C so the correction of flux by water temperature was not considered in this test.

Chemical cleaning and pressure-decay test

Membrane chemical cleaning can be divided into chemically enhanced backwashing (CEB), maintenance cleaning (MC) and restorative cleaning (RC). CEB was performed by injecting chemical cleaning solution into the inner channel of the membrane through the backwashing pump for low concentration chemical backwashing. The flow rate of CEB was the same as the membrane yield. MC was the circulation cleaning method, in other words, the chemical cleaning solution entered the inner channel of the membrane from the filtrate side of the membrane and finally discharged from the water outlet for 30 min chemical cycle cleaning. The RC cleaning method was the same as MC, and its cleaning time was 2 hours. CEB was performed using 200 ppm NaClO solution and 1,000 ppm oxalic acid solution every other day. MC was performed once every 15 days using 1,000 ppm NaClO solution and 2,000 ppm oxalic acid solution. RC was performed once a month using 2,000 ppm NaClO solution and 5,000 ppm oxalic acid solution.

A pressure-decay test (PD) was carried out after each MC. During the test, the membrane was immersed in water, and compressed air at 0.08 MPa was passed into the membrane bore and the pressure was maintained for 10 min.

RESULTS

Effects of additives on the performance of membranes

The mechanical strength and separating performance of HFMs with different additives are summarized in Table 1. PVDF being a hydrophobic material, the water flux of PVDF HFMs was 2.9 L/m^2·h, and the water contact angle was 83° (100/0). When PVDF was blended with PMMA, the membranes obtained better hydrophilicity and the water contact angle dropped to 61° (80/20). When adding additives to PVDF/PMMA system, the contact angle of the membrane decreased and the elongation at break and porosity increased significantly. Meanwhile, the water flux greatly increased with adding 5 wt.% PVP, 5 wt.% PEG1000, and 5 wt.% Tween 80, especially the membrane with 5 wt.% PVP (397.8 L/m^2·h), for which the flux value was six times more than without 5 wt.% PVP. However, its rejection decreased to 79.8%, which was mainly because PVP is more effective in pore formation and can be washed out in the process of modification (Mavukkandy *et al.* 2016).

However, it should be noted that the membrane with 5 wt.% β-CD exhibited excellent performance in rejection (92.2%), although the effect on pure water flux was not obvious. This was owing to the remarkable structure of β-CD, a hollow round table, which has seven α-(1, 4) linked glycosyl units (Yu *et al.* 2015). In addition, β-CD also has a special structure: external hydrophilicity and internal hydrophobicity (Kang & Cao 2014; Liu *et al.* 2020). On the one hand, its multi-hydroxyl structure was easily replaced by other functional groups for better performance and other applications. The circular and multi-hydroxyl structure of β-CD makes it compatible with most polymer chains and it forms hydrogen bonds with the N, O, and F in the polymer, forming a stable supramolecular envelope system (Wang *et al.* 2019; Lu *et al.* 2020; Rahimi *et al.* 2020). The external

Table 1 | Five-bore HFMs characterization with different additives

PVDF/PMMA + additives	Tensile strength (MPa)	Elongation at break (%)	Water flux (L/m^2·h)	Rejection (%)	Porosity (%)	Contact angle (°)
100/0	6.3	18	2.9	–[a]	51.16	83
80/20	8.5	15	60.80	82.4	73.79	61
80/20+5% PVP	10.2	31	397.8	79.8	84.79	40
80/20 5% β-CD	14.1	27	82.7	92.2	83.64	41
80/20 5% PEG	11.2	20	201.6	30.4	80.20	42
80/20 5% Tween 80	10.9	23	187.1	63.6	79.72	45

[a]0.1% BSA aqueous solution cannot pass through the membrane at 0.1 MPa.

hydrophilic structure of β-CD contributes to membrane hydrophilicity (Yu *et al.* 2015; Zhao & Sillanpää 2020).

The Fourier transform infrared spectroscopy (FTIR) spectra of PVDF/β-CD and β-CD is shown in Figure S2. The primary alcohol absorption peak of the PVDF/β-CD blended membrane was at 1,073 cm^{-1}, shifting 43 cm^{-1} from that of pure β-CD, which proved that β-CD was incorporated into the membrane. On the other hand, β-CD has a good solubility in DMAc, thus can be evenly distributed among the polymer molecules. The cross-linking of the polymer formed a polymer chain, and further, a macromolecular network. The polymer network improved the membrane density, making the pure water flux decrease and the rejection increase. Additionally, in the process of membrane preparation, β-CD is washed out and leaves molecular imprinting pores, which also increased the water flux.

Membranes properties with different β-CD content

Five-bore membranes were prepared by adding 5 wt.% PVP and β-CD with a mass fraction of 0, 1, 2, and 3 wt.%, respectively. The total polymer concentration was 17 wt.%, and the ratio of PVDF to PMMA was 4:1 (80/20). The film properties of different combinations of PVP-β-CD additives are shown in Figure 5. When the concentration of β-CD was increased from 0 wt.% to 3 wt.%, the water flux increased from 365.2 LMH to 780.4 LMH. The porosity also increased from 83.65% to 89.29%. When adding 1 wt.% β-CD, the BSA rejection rate increased from 82.6% to 89.7%. However, when the β-CD concentration increased to 3 wt.%, the BSA rejection dropped to 50.20%.

Figure 6 (a1), (a2), (b1), (b2), (c1), (c2), (d1), and (d2) are the SEM micrographs of the outer surface of the membranes with β-CD concentrations of 0, 1, 2, and 3 wt.%, respectively. The SEM photographs (a2), (b2), (c2), and (d2) are magnified 20,000 times. The surface morphologies were homogeneous, with rounded pores and the pore size increased with the increase of β-CD concentration. The surface pores of the membrane with 5 wt.% PVP + 1 wt.% β-CD (Figure 6(b2)) were tiny and dense. They can only be seen clearly when magnified 100,000 times by field emission scanning electron microscopy (Figure 6(b1)).

In the process of membrane preparation, on the one hand, the additives PVP and β-CD, which were compatible with polymer blends, would be partially eluted from the membrane skin layer. In addition, the hydrophilic properties of PVP and β-CD would accelerate the rate of double diffusion of the solvent and the gel precipitate, which caused the membrane pore size to become larger. On the other hand, the additives increased the concentration of the casting solution and reduced the membrane pore size. When only PVP was added and the concentration was less than 5%, the membrane surface pore size increased. When the PVP concentration exceeded 5%, the concentration and viscosity of

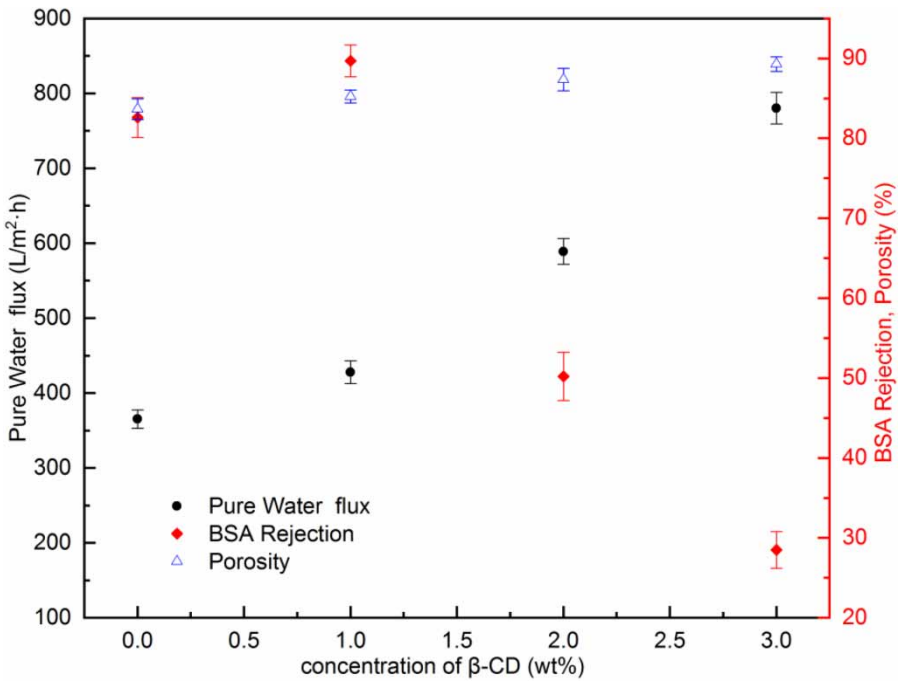

Figure 5 | Variations in water flux, retention rate and porosity of PVDF/PMMA five-bore HFMs with different β-CD concentrations (PVDF:PMMA = 80:20, 5 wt.% PVP).

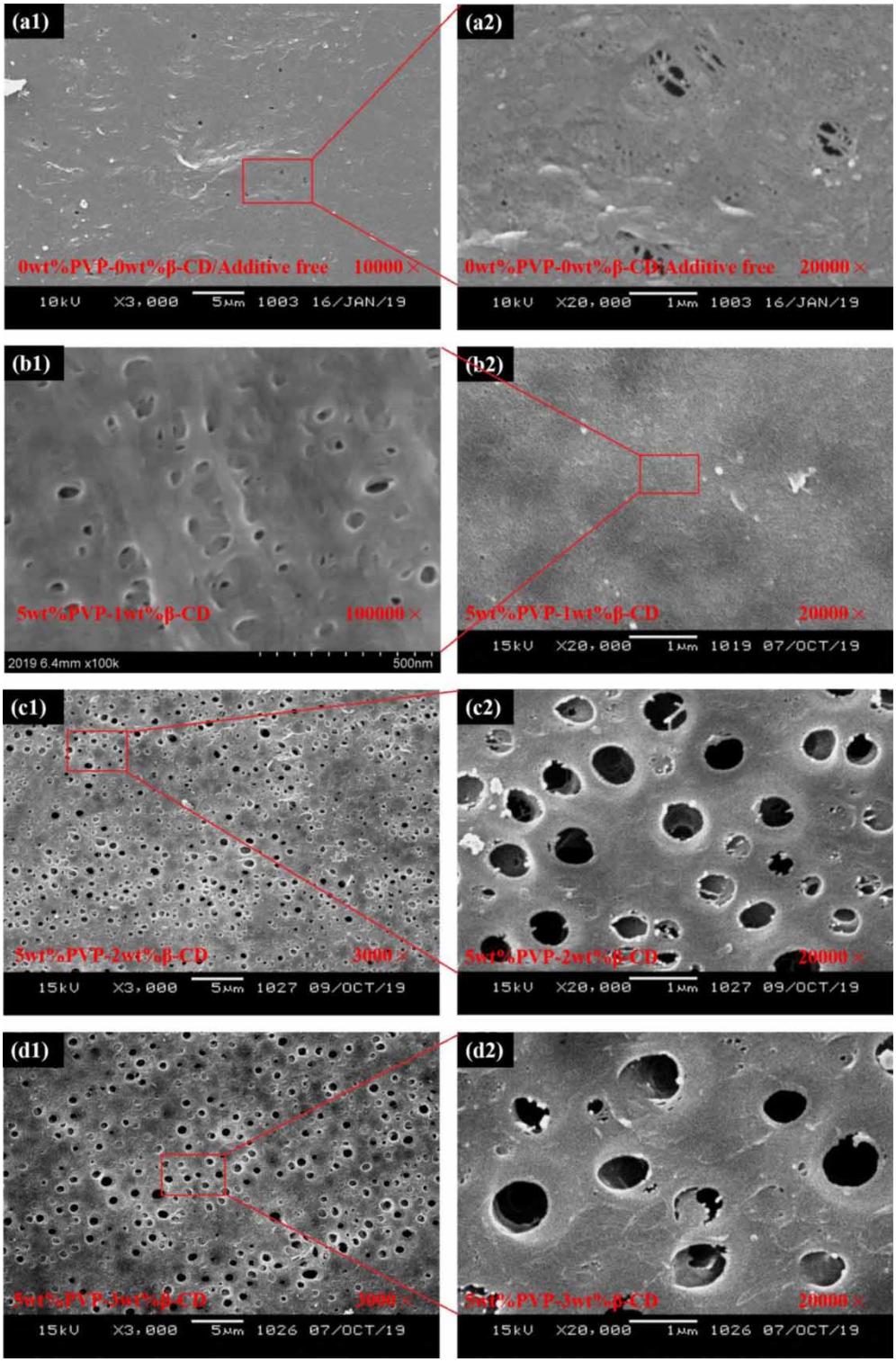

Figure 6 | SEM micrographs of PVDF/PMMA five-bore HFMs with different β-CD concentrations (PVDF:PMMA = 80:20).

the casting solution increased, which reduced the membrane pore size and decreased the water flux (Wu *et al.* 2006; Xu & Xu 2002).

In this experiment, β-CD was introduced, and its hydrophilic hydroxyl groups formed hydrogen bonds with the highly electronegative fluorine atoms in the polymer. At

the same time, it interacted with the solvent and the additive PVP to make it easier for polymer chains to form macromolecular networks, thereby optimizing the membrane porous structure. As shown in Figures 5 and 6, with the increase of β-CD content, the membrane flux continued to increase, and the porosity increased. While when β-CD concentration was 1 wt.%, the maximum BSA rejection rate was obtained, and then it dropped rapidly. Figure 6 shows that when the β-CD concentration was 1 wt.%, the membrane surface pores were the densest, which confirmed Figure 5. Therefore, 1 wt.% β-CD was the best concentration for the blends.

Effect of different additive combination on membranes properties

The total polymer concentration was kept at 17 wt.%, and the mass fraction ratio of PVDF and PMMA was 4:1. The morphological characteristics of the membranes with different additives were observed by SEM. The results are shown in Figure 7. Figure 7(A1), (A2), (B1), (B2), (C1), (C2), (D1), and (D2) are the outer surface of the HFMs without additives, 5 wt.% PVP + 1 wt.% β-CD, 5 wt.% Tween 80 + 1 wt.% β-CD and 5 wt.% PEG + 1 wt.% β-CD, respectively. Of these 5 wt.% PEG + 1 wt.% β-CD (Figure 7(D1), (D2)) was similar to the PVDF/PMMA membrane without additives (Figure 7(A1), (A2)). Both of them have large and sparse surface pores with uneven distribution and irregular shape. It can be seen that the pore distribution of the 5 wt.% Tween 80 + 1 wt.% β-CD membrane (Figure 7(C2)) was linear, which might be related to the distribution of Tween 80 in the casting solution. In addition, a 5 wt.% PVP + 1 wt.% β-CD membrane (Figure 7(B1), (B2) only roughly showed surface pores when the outer surface was magnified 20,000 times. Uniform pores could be seen only when the outer surface was magnified 100,000 times; the average pore diameter was 25 nm (Figure S3).

Figure 7(A3), (B3), (C3), (D3) given an overview of the five-bore membrane cross-sections, and Figure 7(A4), (B4), (C4), (D4) are the profile of the support layer of the

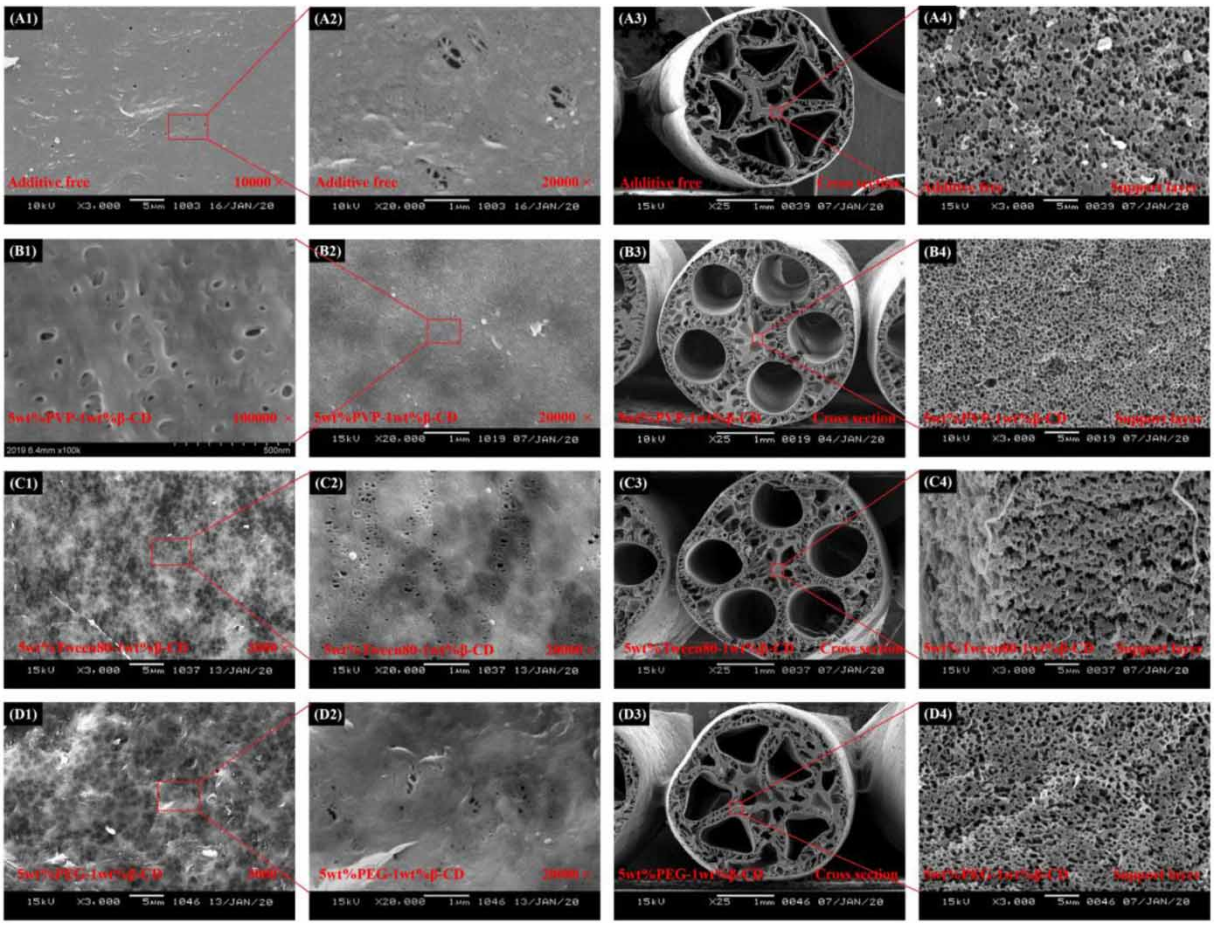

Figure 7 | SEM micrographs of five-bore membranes with different additive combinations PVDF:PMMA = 80:20).

cross-sections. From the SEM photographs, we also observed that the morphologies of membranes without additive (Figure 7(A3)) was similar to 5 wt.% PEG + 1 wt.% β-CD (Figure 7(D3)). They both have five triangular holes, with one angle of each triangle pointing to the center of the membrane. In addition, the structure and morphology of the support layers were similar, with a spongy structure and uneven density, due to similar diffusion rates of water and solvents. In the support layer, the large round, oval or irregular pores were caused by the shrink and stretch of the skin layer during rapid and intense phase inversion in a water-based coagulation bath.

The addition of 5 wt.% PEG + 1 wt.% β-CD increased the polymer concentration, and the permeability of the solvent and non-solvent should be slightly less than that of the base membrane in the process of phase inversion in theory. However, the support layer holes of membrane containing 5 wt.% PEG + 1 wt.% β-CD was smaller than that of the base membrane. It indicated that 5 wt.% PEG + 1 wt.% β-CD improved the porous structure of the membranes.

Figure 7(C3), (C4) shows the membrane of 5 wt.% Tween 80 + 1 wt.% β-CD, and its five holes are circular. The supporting layer was like 5 wt.% PEG + 1 wt.% β-CD, with elliptical and triangular holes. This property increased the porosity and water flux but decreased the strength of the film. We magnified it 3,000 times and observed that its support layer was strip-shaped, sparse and dense sponge structure with filaments in sections.

In Figure 7(B3), (B4), the cross-section of the membrane with 5 wt.% PVP + 1 wt.% β-CD was uniform, and the size of the pores was even and its support layer was a sponge-like structure. Furthermore, the inside and outside of its skin layer were very dense and thin, and on the inside were distributed relatively uniform small finger-like pores. Therefore, the SEM images indicated that PVP combined with β-CD worked well and an appropriate amount of β-CD could improve the porous structure, thus optimizing the membrane in the direction of higher pore density and smaller pore size.

The performances parameters of the membranes with different additive combinations are shown in Table 2. It is clear that the water flux of PVDF/PMMA HFMs was increased significantly when different hydrophilic polymer additives were mixed with β-CD, whereas when 1 wt.% β-CD was mixed with 5 wt.% Tween 80 and 5 wt.% PEG, the rejection of membranes decreased. Comparing the performance of membranes with different additive combinations, it is found that the membranes with 5 wt.% PVP and 1 wt.% β-CD have excellent water permeability, hydrophilicity, retention, and porosity. The obtained water flux was 427.9 L/m^2 h, the contact angle was 25°, the rejection was 89.7% and the porosity was 85.24%.

Table 2 | The properties of multi-bore membranes with different additive combinations

PVDF/PMMA + additives	Water flux (L/m^2·h)	Rejection (%)	Porosity (%)	Contact angle (°)
80/20 + PVP 5% + β-CD 1%	427.9	89.7	85.24	25
80/20 + Tween 80 5% + β-CD 1%	162.3	79.5	76.78	36
80/20 + PEG 5% + β-CD 1%	347.1	27.4	80.45	42

Removal performance of pollutants and membrane operation characteristics

Removal of pollutants from dyeing wastewater

The secondary effluent from dyeing wastewater was deeply treated by HFMs, and the performance of pollutant removal and effluent quality were investigated. The average influent water quality was COD_{cr} 50 mg/L, UV_{254} 0.38 cm^{-1}, turbidity 1.51 NTU, dye concentration 1.04 mg/L, and conductivity 904.5 s/cm. The concentrations of COD_{cr} and UV_{254} in the inlet and outlet water are shown in Figure 8. The content of COD_{cr} and UV_{254} reflected the degree of organic pollution in the water. In the 120 days of operation, with the increase of operation time, the removal rate of COD_{cr} and UV_{254} increased from the 30.7%, 28% to 61.10% and 50.41%, respectively. The fouling layer formed on the membrane surface played the roles of interception and adsorption, which led to better effluent water quality. However, 1–2 days after each chemical cleaning, the effluent water quality would increase temporarily, which was due to the elution of the sediment layer on the membrane surface weakening interception and adsorption.

Turbidity, dye concentration and electrical conductivity of inlet and outlet are shown in Figure 9. With the increase of operation time, turbidity and dye concentration removal rate were continuously improved, and the effluent turbidity and dye concentration were stable at 0.06 NTU and 0.20 mg/L, respectively. In addition, the laboratory-made HFM module had almost no effect on conductivity, which was due to the ultrafiltration membrane having a pore size distribution range of 10–45 nm and basically no desalination function.

Membrane operation and membrane fouling

Membrane fouling occurs at the moment of contact with waste water. The membrane operation of dyeing wastewater

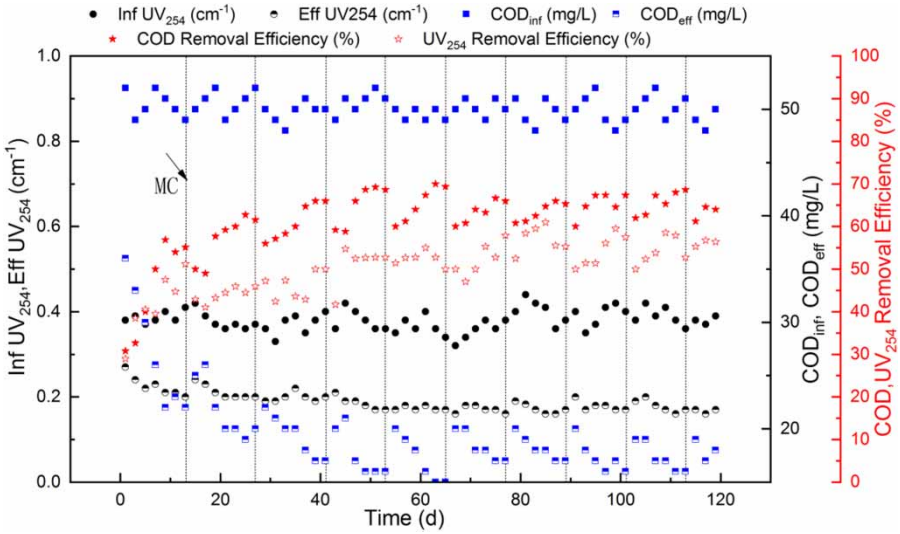

Figure 8 | Variation and removal efficiency of COD_{cr} and UV254 in influent and effluent.

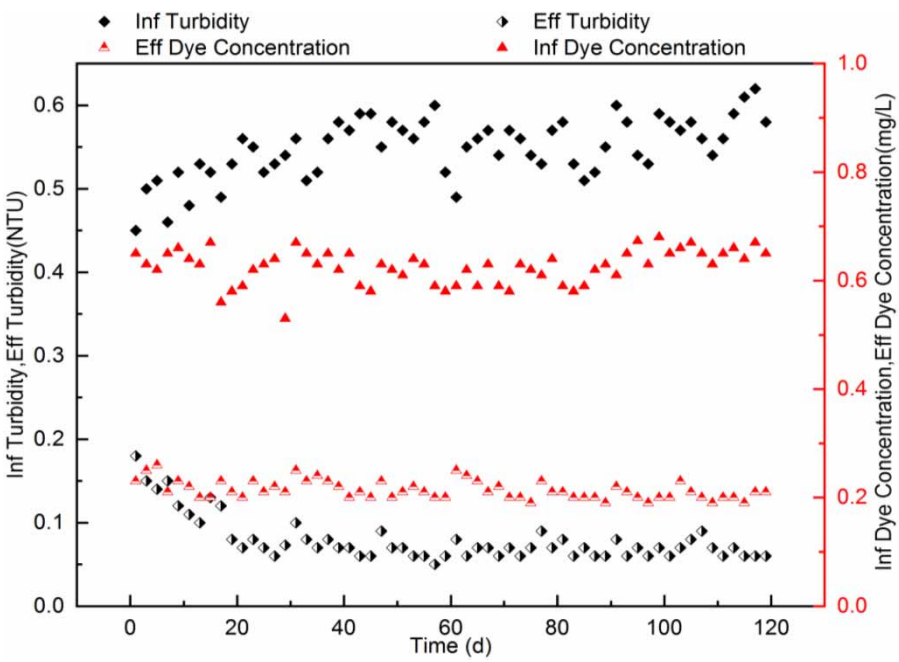

Figure 9 | Variation in turbidity and dye concentration in influent and effluent.

treatment was divided into two stages. In the first stage (1–60 days), the average water flux was 45 LMH. The system recovery was 93.2%, and there was no cross flow. In the second stage (61–120 days), the average water flux and system recovery were 55 LMH and 94%, respectively, and the cross-flow rate was 10%. RC was performed when the SF dropped to 200 LMH/bar. The variations of TMP and SF in the two stages are shown in Figure 10. The second stage improved membrane flux, but the decline rates in TMP and SF in the second stage were slower than in the first stage, indicating that the second stage had a lower membrane fouling rate. Therefore, setting cross flow was more conducive to membrane fouling mitigation. In addition, contaminant removal was stable during the 120 days of operation, and contaminant removal rates were comparable between the two operational phases. Through the pressure-decay test, no breakage and leakage points of the membrane were found, indicating that the mechanical strength of the film was reliable.

The chemical cleaning results showed that CEB and MC can maintain the stable operation of the membrane and

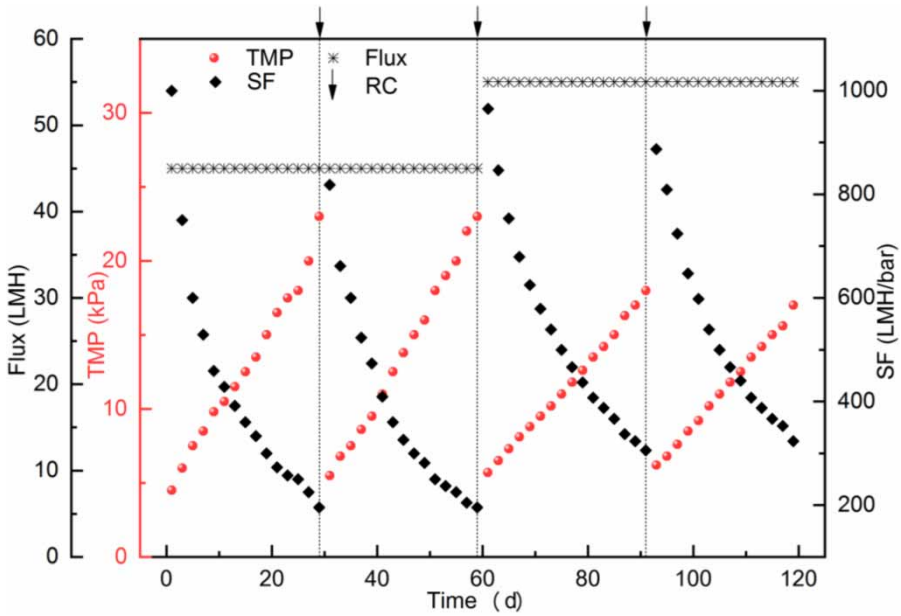

Figure 10 | Variation in TMP, flux, and SF in influent and effluent.

reduce the rate of membrane fouling. As the running time increased, the SF value of the membrane decreased gradually. RC could be used to restore it to 95%. Therefore, RC was a necessary means to ensure the efficient operation of membrane.

CONCLUSIONS

In this work, five-bore HFMs with different additives were synthesized by dry-wet spinning, with a total polymer concentration of 17 wt.%, PVDF/PMMA ratio of 4:1 (80/20). The following conclusions can be summarized from this study:

(1) Through the investigation of the properties of the membranes with different additives, adding 5 wt.% PVP greatly increased water flux and the porosity but decreased the rejection. Adding 5 wt.% β-CD noticeably enhanced tensile strength and rejection of the membrane, without increasing the water flux.

(2) PVDF/PMMA five-bore HFMs were prepared by adding 5 wt.% PVP and different concentrations of β-CD. As the concentration of β-CD increased to 3 wt.%, membrane flux continued to rise, the porosity increased, and BSA rejection increased first and then dropped rapidly. When the β-CD content was 1 wt.%, the optimal membrane performance was obtained. The addition of β-CD makes it easier to form a macromolecular network and improves the surface structure of the membrane.

(3) Different experiments showed that β-CD and PVP were the best additives together. Especially when 5 wt.% PVP was mixed with 1 wt.% β-CD, the best performance of the membrane was the water flux being 427.9 L/m^2·h, the contact angle being 25°, and the retention rate of BSA being 89.7%. It is feasible to prepare ultrafiltration with β-CD and PVP as additives.

(4) The laboratory-made five-hole membrane module effectively removed COD, UV_{254}, turbidity and dye concentration in wastewater. After 120 days of operation, no breaks or leaks were found, showing reliable mechanical properties. The effective membrane operation process to control membrane fouling was: the membrane flux being 55 LMH, with the cross-flow rate being 10%. The periods between CEB, MC and RC were 2 days, 15 days and 30 days, respectively.

ACKNOWLEDGEMENTS

This work was partly funded by PhD innovation fund of North China University of Water Resources and Electric Power

CONFLICTS OF INTEREST

The authors declare no conflict of interest.

DATA AVAILABILITY STATEMENT

All relevant data are included in the paper or its Supplementary Information.

REFERENCES

Aid, S., Eddhahak, A., Khelladi, S., Ortega, Z., Chaabani, S. & Tcharkhtchi, A. 2019 On the miscibility of PVDF/PMMA polymer blends: thermodynamics, experimental and numerical investigations. *Polymer Testing* **73**, 222–231. https://doi:10.1016/j.polymertesting.2018.11.036.

Alsbaiee, A., Smith, B. J., Xiao, L., Ling, Y., Helbling, D. E. & Dichtel, W. R. 2016 Rapid removal of organic micropollutants from water by a porous β-cyclodextrin polymer. *Nature* **529** (7585), 190–194. https://doi.org/10.1038/nature16185.

Amirilargani, M., Saljoughi, E. & Mohammadi, T. 2009 Effects of Tween 80 concentration as a surfactant additive on morphology and permeability of flat sheet polyethersulfone (PES) membranes. *Desalination* **249** (2), 837–842. https://doi.org/10.1016/j.desal.2009.01.041.

Back, J., Brandstätter, R., Spruck, M., Koch, M., Penner, S. & Rupprich, M. 2019 Parameter screening of PVDF/PVP multi-channel capillary membranes. *Polymers* **11** (3), 463. https://doi:10.3390/polym11030463.

Bagheri, M. & Mirbagheri, S. A. 2018 Critical review of fouling mitigation strategies in membrane bioreactors treating water and wastewater. *Bioresource Technology.* **258**, 318–334. https://doi:10.1016/j.biortech.2018.03.026.

Bi, Q., Li, Q., Tian, Y., Lin, Y. & Wang, X. 2012 Hydrophilic modification of poly(vinylidene fluoride) membrane with poly(vinyl pyrrolidone) via a cross-linking reaction. *Journal of Applied Polymer Science* **127** (1), 394–401. https://doi.org/10.1002/app.37629.

Bu-Rashid, K. A. & Czolkoss, W. 2007 Pilot tests of multibore UF membrane at Addur SWRO desalination plant, Bahrain. *Desalination* **203** (1–3), 229–242. https://doi.org/10.1016/j.desal.2006.04.010.

Chakrabarty, B., Ghoshal, A. K. & Purkait, M. K. 2008 Effect of molecular weight of PEG on membrane morphology and transport properties. *Journal of Membrane Science* **309** (1–2), 209–221. https://doi.org/10.1016/j.memsci.2007.10.027.

Chang, H.-H., Chen, S.-C., Lin, D.-J. & Cheng, L.-P. 2014 The effect of Tween-20 additive on the morphology and performance of PVDF membranes. *Journal of Membrane Science* **466**, 302–312. https://doi.org/10.1016/j.memsci.2014.05.011.

Crini, G. 2014 Review: a history of cyclodextrins. *Chemical Reviews* **114** (21), 10940–10975. https://doi:10.1021/cr500081p.

Gao, N., Yang, J., Wu, Y., Yue, J., Cao, G., Zhang, A., Ye, L. & Feng, Z. 2019 *β*-Cyclodextrin functionalized coaxially electrospun poly(vinylidene fluoride) @ polystyrene membranes with higher mechanical performance for efficient removal of phenolphthalein. *Reactive and Functional Polymers* **141**, 100–111. https://doi.org/10.1016/j.reactfunctpolym.2019.05.001.

Huang, C. & Zhang, L. 2004 Miscibility of poly(vinylidene fluoride) and atactic poly(methyl methacrylate). *Journal of Applied Polymer Science* **92** (1), 1–5. https://doi.org/10.1002/app.13564.

Huang, J., Luo, Y., Xi, D. & Liu, N. 2009 Removal of polycyclic aromatic hydrocarbons by the membrane improved with cyclodextrine. In *2009 3rd International Conference on Bioinformatics and Biomedical Engineering*. iCBBE, pp. 1–4. https://doi:10.1109/icbbe.2009.5163314.

Kang, G. D. & Cao, Y. M. 2014 Application and modification of poly (vinylidene fluoride) (PVDF) membranes – A review. *Journal of Membrane Science* **463** (1), 145–165. https://doi.org/10.1016/j.memsci.2014.03.055.

Khayet, M., Feng, C. Y., Khulbe, K. C. & Matsuura, T. 2002 Preparation and characterization of polyvinylidene fluoride hollow fiber membranes for ultrafiltration. *Polymer* **43** (14), 3879–3890. http://doi.org/10.1016/S0032-3861(02)00237-9.

Li, X., Ang, W. L., Liu, Y. & Chung, T.-S. 2015 Engineering design of outer-selective tribore hollow fiber membranes for forward osmosis and oil-water separation. *AIChE Journal* **61** (12), 4491–4501. https://doi:10.1002/aic.15012.

Liu, F., Xu, Y. Y., Zhu, B. K., Zhang, F. & Zhu, L. P. 2009 Preparation of hydrophilic and fouling resistant poly(vinylidene fluoride) hollow fiber membranes. *Journal of Membrane Science* **345** (1–2), 331–339. https://doi.org/10.1016/j.memsci.2009.09.020.

Liu, F., Hashim, N. A., Liu, Y., Abed, M. R. M. & Li, K. 2011 Progress in the production and modification of PVDF membranes. *Journal of Membrane Science* **375** (1–2), 1–27. https://doi:10.1016/j.memsci.2011.03.014.

Liu, Q., Zhou, Y., Lu, J. & Zhou, Y. 2020 Novel cyclodextrin-based adsorbents for removing pollutants from wastewater: a critical review. *Chemosphere* **241**, 125043. https://doi.org/10.1016/j.chemosphere.2019.125043.

Loukidou, M. X. & Zouboulis, A. I. 2001 Comparison of two biological treatment processes using attached-growth biomass for sanitary landfill leachate treatment. *Environment Pollution* **111** (2001), 273–281. https://doi:10.1016/s0269-7491(00)00069-5.

Lu, J., Qin, Y.-Y. , Wu, Y.-L., Chen, M.-N., Sun, C., Han, Z.-X., Yan, Y.-S., Li, C.-X. & Yan, Y. 2020 Mimetic-core-shell design on molecularly imprinted membranes providing an antifouling and high-selective surface. *Chemical Engineering Journal*, 128085. http://doi:10.1016/j.cej.2020.128085.

Lu, K.-J., Zuo, J. & Chung, T.-S. 2016 Tri-bore PVDF hollow fibers with a super-hydrophobic coating for membrane distillation. *Journal of Membrane Science* **514**, 165–175. https://doi.org/10.1016/j.memsci.2016.04.058.

Luo, L., Wang, P., Zhang, S., Han, G. & Chung, T. S. 2014 Novel thin-film composite tri-bore hollow fiber membrane fabrication for forward osmosis. *Journal of Membrane Science* **461**, 28–38. https://doi.org/10.1016/j.memsci.2014.03.007.

Ma, C. Y., Huang, J. P. & Xi, D. L. 2012 Preparation, characterization and performance of a novel PVDF/PMMA/TPU blend hollow fiber membrane for wastewater treatment. *Water Science and Technology* **65** (6), 1041–1047. https://doi:10.2166/wst.2012.930.

Ma, T., Cui, Z., Wu, Y., Qin, S., Wang, H., Yan, F., Han, N. & Li, J. 2013 Preparation of PVDF based blend microporous membranes for lithium ion batteries by thermally induced phase separation: I. Effect of PMMA on the membrane formation process and the properties. *Journal of Membrane Science* **444**, 213–222. https://doi.org/10.1016/j.memsci.2013.05.028.

Ma, C., Wu, X. & Liu, Z. 2016 Performance and fouling characterization of a five-bore hollow fiber membrane in a membrane bioreactor for the treatment of printing and dyeing wastewater. *Textile Research Journal* **87** (1), 102–109. https://doi:10.1177/0040517515624876.

Marchese, J., Ponce, M., Ochoa, N. A., Prádanos, P., Palacio, L. & Hernández, A. 2003 Fouling behaviour of polyethersulfone UF membranes made with different PVP. *Journal of Membrane Science* **211** (1), 1–11. https://doi.org/10.1016/S0376-7388(02)00260-0.

Mavukkandy, M. O., Bilad, M. R., Giwa, A., Hasan, S. W. & Arafat, H. A. 2016 Leaching of PVP from PVDF/PVP blend membranes: impacts on membrane structure and fouling in membrane bioreactors. *Journal of Materials Science* **51**, 4328–4341. https://doi:10.1007/s10853-016-9744-7.

Okabe, Y., Murakami, H., Osaka, N. & Saito, H. 2010 Morphology development and exclusion of noncrystalline polymer during crystallization in PVDF/PMMA blends. *Polymer* **51** (6), 1494–1500. https://doi.org/10.1016/j.polymer.2010.01.055.

Pan, B., Zhu, L. & Li, X. 2013 Preparation of PVDF/$CaCO_3$ composite hollow fiber membrane via a thermally induced phase separation method. *Polymer Composites* **34** (7), 1204–1210. https://doi.org/10.1002/pc.22532.

Peng, N., Teoh, M. M., Chung, T. S. & Koo, L. L. 2011 Novel rectangular membranes with multiple hollow holes for ultrafiltration. *Journal of Membrane Science* **372** (1–2), 20–28. https://doi.org/10.1016/j.memsci.2011.01.022.

Rahimi, Z., Zinatizadeh, A. A., Zinadini, S. & van Loosdrecht, M. C. M. 2020 β-cyclodextrin functionalized MWCNTs as a promising antifouling agent in fabrication of composite nanofiltration membranes. *Separation and Purification Technology*. **247**, 116979. https://doi.org/10.1016/j.seppur.2020.116979.

Rajabzadeh, S., Liang, C., Ohmukai, Y., Maruyama, T. & Matsuyama, H. 2012 Effect of additives on the morphology and properties of poly(vinylidene fluoride) blend hollow fiber membrane prepared by the thermally induced phase separation method. *Journal of Membrane Science* **423–424**, 189–194.

Simone, S., Figoli, A., Criscuoli, A., Carnevale, M. C., Rosselli, A. & Drioli, E. 2010 Preparation of hollow fibre membranes from PVDF/PVP blends and their application in VMD. *Journal of Membrane Science* **364** (1–2), 219–232. https://doi.org/10.1016/j.memsci.2010.08.013.

Wan, P., Yin, J. & Deng, B. 2017 Seven-bore hollow fiber membrane (HFM) for ultrafiltration (UF). *Chemical Engineering Research and Design* **128**, 240–247. https://doi.org/10.1016/j.cherd.2017.09.019.

Wang, P. & Chung, T. S. 2012 Design and fabrication of lotus-root-like multi-bore hollow fiber membrane for direct contact membrane distillation. *Journal of Membrane* **421–422**, 361–374. https://doi.org/10.1016/j.memsci.2012.08.003.

Wang, P., Luo, L. & Chung, T. S. 2014 Tri-bore ultra-filtration hollow fiber membranes with a novel triangle-shape outer geometry. *Journal of Membrane Science* **452**, 212–218. https://doi.org/10.1016/j.memsci.2013.10.033.

Wang, Z., Zhang, B., Fang, C., Liu, Z., Fang, J. & Zhu, L. 2019 Macroporous membranes doped with micro-mesoporous β-cyclodextrin polymers for ultrafast removal of organic micropollutants from water. *Carbohydrate Polymers* **222**, 114970. https://doi:10.1016/j.carbpol.2019.114970.

Wongchitphimon, S., Wang, R., Jiraratananon, R., Shi, L. & Loh, C. H. 2011 Effect of polyethylene glycol (PEG) as an additive on the fabrication of polyvinylidene fluoride-co-hexafluoropropylene (PVDF-HFP) asymmetric microporous hollow fiber membranes. *Journal of Membrane Science* **369** (1–2), 329–338. https://doi.org/10.1016/j.memsci.2010.12.008.

Wu, L., Sun, J. & Wang, Q. 2006 Poly(vinylidene fluoride)/polyethersulfone blend membranes: effects of solvent sort, polyethersulfone and polyvinylpyrrolidone concentration on their properties and morphology. *Journal of Membrane Science* **285** (1–2), 290–298. https://doi.org/10.1016/j.memsci.2006.08.033.

Wu, H., Tang, B. & Wu, P. 2013 Preparation and characterization of anti-fouling β-cyclodextrin/polyester thin film nanofiltration composite membrane. *Journal of Membrane Science* **428**, 301–308. https://doi.org/10.1016/j.memsci.2012.09.063.

Xu, J. & Xu, Z.-L. 2002 Poly(vinyl chloride) (PVC) hollow fiber ultrafiltration membranes prepared from PVC/additives/solvent. *Journal of Membrane Science* **208** (1–2), 203–212. https://doi.org/10.1016/S0376-7388(02)00261-2.

Yin, J., Zhu, G. & Deng, B. 2013 Multi-walled carbon nanotubes (MWNTs)/polysulfone (PSU) mixed matrix hollow fiber membranes for enhanced water treatment. *Journal of Membrane Science* **437**, 237–248. https://doi.org/10.1016/j.memsci.2013.03.021.

Yu, Z., Pan, Y., He, Y., Zeng, G., Shi, H. & Di, H. 2015 Preparation of a novel anti-fouling β-cyclodextrin-PVDF membrane. *RSC Advances* **5** (63), 51364–51370. https://doi:10.1039/c5ra04894j.

Zhang, Y., Qin, C. & Binner, J. 2006 Processing multi-channel alumina membranes by tape casting latex-based suspensions. *Ceramics International* **32** (7), 811–818. https://doi.org/10.1016/j.ceramint.2005.06.005.

Zhang, P.-Y., Xu, Z.-L., Ma, X.-H., Yang, H., Wu, W.-Z., Wei, Y.-M. & Liu, Y.-D. 2015 Fabrication and characterization of PVDF hollow fiber membranes employing in-situ self-assembly modulation concept. *Journal of Membrane Science* **486**, 119–131. https://doi.org/10.1016/j.memsci.2015.03.051.

Zhang, B., Huang, D. M., Shen, Y., Yin, W., Gao, X., Zhang, B. & Shi, W. 2020 Treatment of municipal wastewater with aerobic granular sludge membrane bioreactor (AGMBR): performance and membrane fouling. *Journal of Cleaner Production* **273**, 123124. https://doi.org/10.1016/j.jclepro.2020.123124.

Zhao, F. & Sillanpää, M. 2020 Chapter 3 - cross-linked chitosan and β-cyclodextrin as functional adsorbents in water treatment. *Advanced Water Treatment* 161–264. https://doi.org/10.1016/B978-0-12-819216-0.00003-5.

Zhou, Y. & Xi, D.-L. 2008 Porous PVDF/TPU blends asymmetric hollow fiber membranes prepared with the use of hydrophilic additive PVP (K30). *Desalination* **223** (1–3), 438–447. https://doi.org/10.1016/j.desal.2007.01.184.

First received 18 November 2020; accepted in revised form 9 March 2021. Available online 19 March 2021